February 2006

A Bidomain Nonribosomal Peptide Synthetase Encoded by *FUM14* Catalyzes the Formation of Tricarballylic Esters in the Biosynthesis of Fumonisins

Kathia Zaleta-Rivera

Chunping Xu

Fengan Yu

Robert A. E. Butchko

Robert H. Proctor

See next page for additional authors

Authors

Kathia Zaleta-Rivera, Chunping Xu, Fengan Yu, Robert A. E. Butchko, Robert H. Proctor, Maria E. Hidalgo-Lara, Ashraf S. Raza, Patrick Dussault, and Liangcheng Du

A Bidomain Nonribosomal Peptide Synthetase Encoded by *FUM14* Catalyzes the Formation of Tricarballylic Esters in the Biosynthesis of Fumonisins[†]

Kathia Zaleta-Rivera,[‡,§] Chunping Xu,[‡] Fengan Yu,[‡] Robert A. E. Butchko,[||] Robert H. Proctor,[||] María E. Hidalgo-Lara,[§] Ashraf Raza,[⊥] Patrick H. Dussault,[‡] and Liangcheng Du*,[‡]

Departments of Chemistry and Biochemistry, University of Nebraska−Lincoln, Lincoln, Nebraska 68588, National Center for Agriculture Utilization Research, ARS-USDA, 1815 North University Street, Peoria, Illinois 61604, and Departamento de Biotecnología y Bioingeniería, CINVESTAV−IPN, Col. Zacatenco, CP 07360, Mexico D.F., Mexico

ABSTRACT: Fumonisins are a group of polyketide-derived mycotoxins produced by *Fusarium verticillioides*, a filamentous fungus infecting corn and contaminating food and feeds. Fumonisins contain two tricarballylic esters that are critical for toxicity. Here, we present genetic and biochemical data for the esterification mechanism. *FUM14* in *F. verticillioides* has been deleted by homologous recombination, and the resultant mutant lost the ability to produce fumonisins. Two new metabolites, HFB$_3$ and HFB$_4$, which are biosynthetic precursors of fumonisins lacking the tricarballylic esters, were detected in the mutant. The results suggest that *FUM14* is required for the esterification of fumonisins. *FUM14* was predicted to encode a nonribosomal peptide synthetase (NRPS) containing two domains, peptidyl carrier protein and condensation domain. Both the intact Fum14p and the condensation domain have been expressed in *Escherichia coli* and purified for activity assays. Fum14p was able to convert HFB$_3$ and HFB$_4$ to the tricarballylic esters-containing fumonisins, FB$_3$ and FB$_4$, respectively, when incubated with tricarballylic thioester of *N*-acetylcysteamine. In addition, the condensation domain was able to convert HFB$_1$ to FB$_1$. These data provide direct evidence for the role of Fum14p in the esterification of fumonisins. More interestingly, the results are the first example of an NRPS condensation domain catalyzing a C−O bond (ester) formation, instead of the typical C−N bond (amide) formation in nonribosomal peptides. The understanding of the esterification mechanism provides useful knowledge for mycotoxin reduction and elimination. The study also provides new insight into the reactions catalyzed by NRPS.

Fumonisins are polyketide-derived mycotoxins produced by several filamentous fungi, including *Fusarium verticillioides*, which is a widespread pathogen of corn (*1, 2*). These mycotoxins are structurally similar to the long-chain base of sphingolipids and thus can disrupt the sphingolipid pathway by inhibiting sphinganine *N*-acyltransferase (ceramide synthase) (*3*). This disruption is thought to be responsible for several fatal animal diseases, such as leukoencephalomalacia in horses and pulmonary edema in pigs, and the epidemiological association of fumonisins and esophageal cancer and neural tube defects in humans (*1, 4, 5*). The fungus is associated with disease at all stages of maize plant development, infecting the roots, stalk, and kernels. Wild-type strains of the fungus predominantly produce the B-series fumonisins, including fumonisin B$_1$ (FB$_1$),[1] fumonisin B$_2$ (FB$_2$), fumonisin B$_3$ (FB$_3$), and fumonisin B$_4$ (FB$_4$) (Figure 1).
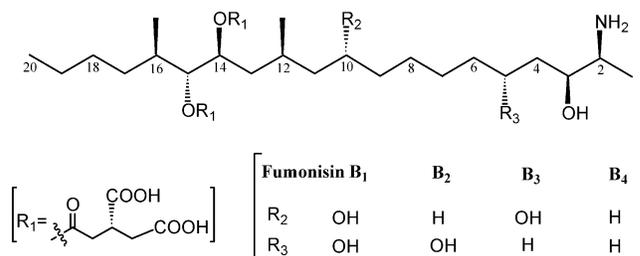

FIGURE 1: Chemical structure of the B-series fumonisins.

The chemical structure of fumonisins is characterized by having two tricarballylic esters on the carbon backbone (Figure 1) (*2, 6*). The esterification is an essential step in the maturation of fumonisins, because without the esters the mycotoxins are not fully active (*7−9*). The esters are formed between a tricarboxylic acid (propane-1,2,3-tricarboxylic acid) and the hydroxyls at C-14 and C-15 of the fumonisin backbone (Figure 1). Previous studies using ^{13}C-enriched

* To whom correspondence should be addressed at Department of Chemistry, University of Nebraska, 729 Hamilton Hall, Lincoln, NE 68588. Phone, 1-402-472-2998; fax, 1-402-472-9402; e-mail, ldu@unlserve.unl.edu.
‡ Department of Chemistry, University of Nebraska−Lincoln.
§ CINVESTAV−IPN.
|| ARS-USDA.
⊥ Department of Biochemistry, University of Nebraska−Lincoln.

[1] Abbreviations: C, condensation; CoA, coenzyme A; EDTA, ethylenediaminetetraacetic acid; ELSD, evaporative light-scattering detection; FB, Fumonisin B series; HPLC, high-performance liquid chromatography; IPTG, β-isopropyl-thiogalactoside; ESIMS, electrospray ionization mass spectrometry; MBP, maltose binding protein; NRPS, nonribosomal peptide synthetase; PCP, peptidyl carrier protein; PCR, polymerase chain reaction; SDS−PAGE, sodium dodecyl sulfate−polyacrylamide gel electrophoresis; SNAC, thioester of *N*-acetylcysteamine; TCA, tricarballylic acid.

substrates suggested that the precursor for the tricarballylic esters may be an intermediate from the Krebs Cycle (*10*). However, the biosynthetic mechanism for the ester formation is not clear.

Proctor et al. identified a 15-gene cluster (*FUM*) responsible for the biosynthesis of fumonisins in *F. verticillioides* (*11*). On the basis of the sequence annotation and preliminary results from gene deletion experiments, Butchko et al. have proposed that three genes, *FUM7*, *FUM10*, and *FUM14*, are involved in the formation of the esters (*12*). The deduced amino acid sequence of *FUM10* is similar to acyl-CoA synthetase and the adenylation domain of nonribosomal peptide synthetase (NRPS); the deduced amino acid sequence of *FUM14* is similar to the peptidyl carrier protein (PCP) and condensation domain (C) of NRPS (*13*), and the deduced amino acid sequence of *FUM7* is similar to dehydrogenases, which could be regarded as a reductase domain of NRPS (*14*, *15*). Thus, *FUM7*, *FUM10*, and *FUM14* may encode enzymes that make up an NRPS complex.

In NRPS, the adenylation domain activates an amino acid and transfers it to PCP as a covalently linked thioester via a 4′-phosphopantetheinyl cofactor (*13*, *16*). The C domain then catalyzes the condensation reaction between the acyl thioesters on PCP to form an amide (C−N) bond. Therefore, among the four genes, *FUM14* is the most likely candidate that is directly involved in the transfer of the acyl groups to the hydroxyls on polyketide backbone. The *FUM14* protein (Fum14p) could catalyze formation of the ester C−O bonds in the biosynthesis of fumonisins. A C−O bond formation catalyzed by an NRPS condensation domain has not been reported in the biosynthesis of nonribosomal peptides. Therefore, the characterization of *FUM14* not only helps reveal the biosynthetic mechanism for the side-chain formation of fumonisins but also could shed new light on the reactions catalyzed by NRPS. Here, we report the gene disruption and heterologous expression of *FUM14* and in vitro activity assays for the purified Fum14p.

EXPERIMENTAL PROCEDURES

General DNA Manipulations. Plasmids preparation and DNA extraction were carried out by using commercial kits (Qiagen, Valencia, CA), and all other manipulations were carried out according to standard methods (*17*). *Escherichia coli* DH5α strain was used as the host for general DNA propagations, and the pGEM-zf vector series from Promega (Madison, WI) was used for cloning and DNA sequencing. Genomic DNA of *F. verticillioides* was prepared as described previously (*18*).

Construction of FUM14 Deletion Vector pUCH2-F14. To construct the *FUM14* vector, two DNA fragments were amplified by PCR from Cos4-5 (*11*), which contains most of the *FUM* gene cluster including *FUM13*, *FUM14*, and *FUM15* (see Figure 2). A 991-bp fragment (left-side arm), which covers the noncoding region downstream to *FUM14* and the 3′-region of *FUM13*, was amplified by using primers PLF/PLR (Table 1). A 1087-bp fragment (right-side arm), which covers the 5′-region of *FUM14* and the noncoding region upstream to *FUM14*, was amplified by using primers PRF/PRR (Table 1). The right-side arm was digested with *Hind*III and *Bam*HI and cloned into plasmid pUCH2-8, which carries a hygromycin B resistance gene (*HygB*) (*19*).

The left-side arm was digested with *Apa*I/*Sal*I to generate an 834-bp fragment, which was subsequently cloned into the *Apa*I/*Sal*I site of the above construct. This generated a 7.3-kb plasmid, pUCH2-F14, in which the *HygB* gene is flanked by the left-side arm and right-side arm as shown in Figure 2. The plasmid was used to create *FUM14*-deleted mutants by homologous recombination at the left-side and right-side arms.

Transformation of F. verticillioides and Screening for Mutants. The procedure for *F. verticillioides* protoplast isolation and transformation was essentially identical to that described previously (*20*). Briefly, the plasmid DNA (5 μg) was diluted with STC buffer (100 μL final) and mixed with protoplasts (100 μL), and transformation was mediated with PEG 8000 buffer (30% PEG 8000, 10 mM Tris-HCl, pH 8.0, and 50 mM CaCl$_2$). Hygromycin-resistant colonies were selected on YPD plates containing hygromycin B (150 μg/mL, Calbiochem, La Jolla, CA). Three different pairs of primers were used in PCR to identify the *FUM14*-deleted mutants from the hygromycin resistant colonies. First, a pair of primers binding to *HygB* was used to verify that the colonies contained this gene. Then, two pairs of primers (P1/P2 and P3/P4, see Table 1 for sequences) were used to verify that colonies positive for *HygB* resulted from homologous recombination at the flanking regions of *FUM14*, but not from a random integration of the plasmid. Primer P1 binds to a region that is outside of the left-side arm, whereas primer P2 binds to the *HygB* gene (Figure 2). Therefore, only the colonies resulting from homologous recombination at the left-side arm could yield a PCR product of the expected size, whereas colonies containing a randomly integrated vector or resulting from rearrangement after the homologous recombination would not yield this specific product. Similarly, primers P3/P4 were used to confirm the homologous recombination at the right-side arm (Figure 2). Thus, *FUM14*-deleted mutants were identified from colonies that yielded the PCR product expected for homologous recombination on both the left-side and right-side arms.

Production and Extraction of Metabolites from Mutants. The mutant strains were transferred separately to a YPD/hygromycin (300 μg/mL) plate to generate single colonies. A single colony was then transferred to a 10 mL tube containing 3 mL of YPD/hygromycin (150 μg/mL) liquid medium and allowed to grow in a shaker (60 rpm) at room temperature for 2 days. From the 3 mL culture, 100 μL was transferred to a flask containing 25 mL of YPD/hygromycin (150 μg/mL). The culture was incubated with shaking at room temperature for another 2 days. The culture was transferred to a 50 mL tube and centrifuged at 2500 rpm for 20 min. The pellet was washed three times with sterile water and finally resuspended in 10 mL of sterile water. From the suspended solution, 500 μL was transferred to a new flask containing 10 g of autoclaved CMK (Cracked Maize Kernels) medium (*11*). Alternatively, colonies derived from single spores of the mutants were inoculated on V8 agar plates. After 1-week growth at room temperature, spores were collected from the plates and used to inoculate the 10 g CMK medium. After 3 weeks of incubation at room temperature in the dark, metabolites were extracted from the CMK cultures with 20 mL of 50% acetonitrile. The extracts were filtered, and a sample of 50 μL was injected in HPLC−ELSD to analyze the metabolites.
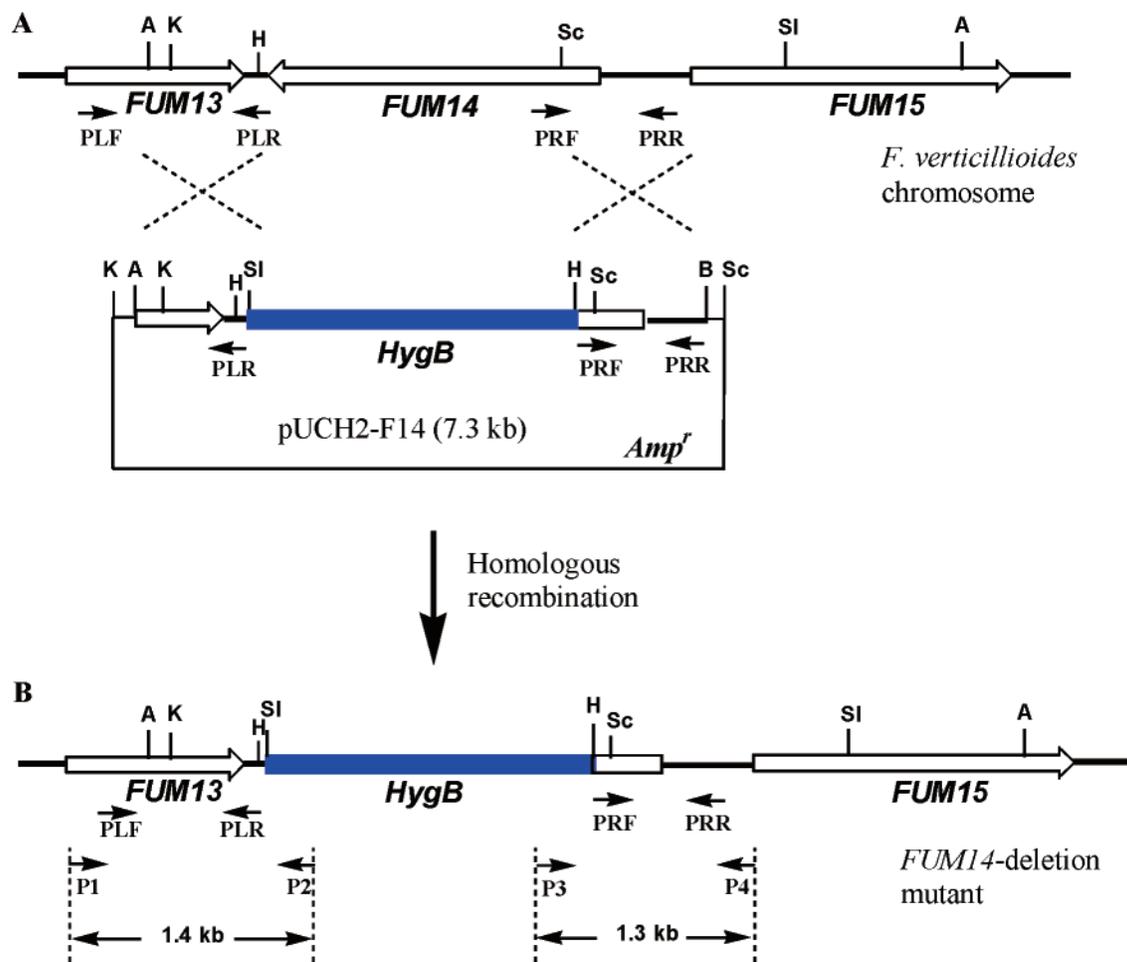
FIGURE 2: The construction of *FUM14* gene deletion vector and screening of the *FUM14*-deleted mutants. (A) Homologous recombination between *FUM14* on the *F. verticillioides* chromosome and the homologous sequences on plasmid pUCH2-F14. The positions for PCR primer binding sites are indicated by small arrows. Abbreviations: A, *Apa*I; B, *Bam*HI; H, *Hind*III; K, *Kpn*I; Sc, *Sac*I; Sl, *Sal*I; *HygB*, hygromycin B resistant gene. (B) Gene-replacement mutants resulted from double crossovers at the upstream homologous region (left-side arm) and at the downstream homologous region (right-side arm). The expected size for PCR products is indicated below the corresponding genes.

Table 1: Primers Used in the Experiments

name	sequences
PLF	5′-CCG CTC GAG TAT TAC AAG GGC GAC TC-3′
PLR	5′-CGC GTC GAC GAT AGC TAG AGC ATA TTC GG-3′
PRF	5′ CGT GAA GCT TGG GAA CTC GTC CTT TCT-3′
PRR	5′CGC GGA TCC GAA GCA CAG AGT CGG AAA ACG-3′
P1	5′-GTA CAA GCA CGG ACT TGA AAG AG-3′
P2	5′-GAT GTG TTA GAA GCT CAC AGA AGG-3′
P3	5′-CAT AAC CAA GCC TAT GCC TAC AG-3′
P4	5′-GCA TAC TGC CTG TTC TAG GAT TG-3′
F14-C-F	5′-CGC GGA TCC TTG CCT TTA TGG TCT ATG-3′
F14-C-R	5′-CCC AAG CTT CTA GTC CAA CAA GCC TGT-3′
F14-F	5′-CGC GGA TCC AAT TCA TTG GAC CAG TGG-3′
F14-R	5′-CCG CTC GAG CTA GTC CAA CAA GCC TGT-3′

Construction of Expression Vectors. To construct the expression vector that contained the C domain alone (Fum14-C), a 1.3 kb fragment of *FUM14* carrying the domain was amplified by PCR from the genomic DNA of *F. verticillioides* with primers F14-C-F and F14-C-R (Table 1). High-fidelity DNA polymerase *Pfu* (Stratagene) was used in the reactions. The PCR fragment was digested with *Bam*HI and *Hind*III and cloned into pGEM-3zf. After sequence fidelity of the amplification product was confirmed by DNA sequencing, it was transferred to expression vector pMAL-c2 (New England BioLabs), which is designed to yield the expressed protein fused to the maltose-binding protein (MBP).

To construct the complete Fum14p expression vector, a 1.6 kb fragment was amplified by PCR from a cDNA library of *F. verticillioides* using the forward primer F14-F and a reverse primer F14-R (Table 1). The PCR fragment was digested with *Bam*HI and *Xho*I and cloned into pT7Blue-3. After confirmation by DNA sequencing, the gene was transferred to expression vector pMAL-c2 as described above.

Expression and Purification of Fum14-C and Fum14-PCP-C. E. coli TB1 (New England BioLabs) strain was used for expression from the pMAL-based constructs. The standard conditions for cell growth and expression induction were followed as recommended by the manufacturer. The cells were incubated in a shaker (250 rpm) at 25 °C until the cell density reached 0.6 at OD_{600nm}. To induce the expression of *FUM14*, IPTG (0.1 mM) was added to the culture, and the cells were allowed to grow at the same conditions for another 3 h. The soluble fraction of the overproduced proteins was loaded to an amylose resin column (BioLabs) for affinity purification of the proteins. The purified proteins were desalted on a PD-10 column (Pharmacia Biotech, Piscataway, NJ), eluted in 50 mM Tris-HCl buffer, pH 8.0, containing
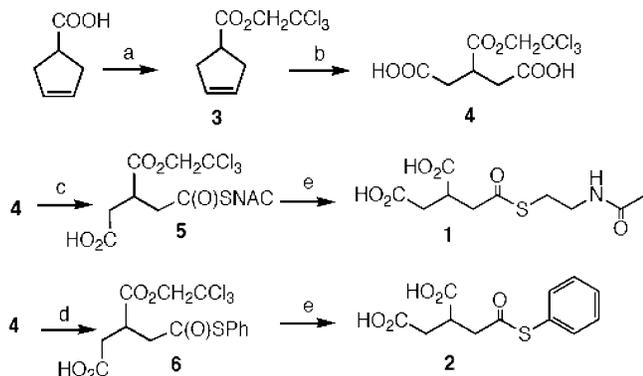
FIGURE 3: Synthesis of TCA thioesters. (a) CCl_3CH_2OH, DCC, pyridine; (b) $RuCl_3$, $NaIO_4$; (c) *N*-acetylcysteamine, DCC, pyridine; (d) thiophenol, DCC, pyridine; (e) Zn/HOAc.

200 mM NaCl, 10 mM $MgCl_2$, 2 mM dithiothreitol (DTT), 1 mM EDTA, and 10% glycerol, and stored at −80 °C for in vitro assays.

Preparation of HFB$_1$, HFB$_3$, and HFB$_4$. The preparation of the hydrolyzed FB$_1$ (HFB$_1$) and hydrolyzed FB$_3$ (HFB$_3$) was conducted by using the alkaline method (*21*). Approximately 2 mg of fumonisins was refluxed in 2.5 mL of 0.25 N potassium hydroxide for 24 h. The solution was acidified to pH 5 with 2 N HCl and analyzed by HPLC−ELSD. The hydrolyzed fumonisin was purified by HPLC and dried under vacuum. Alternatively, HFB$_3$ and HFB$_4$ were prepared from the culture of *FUM14*-deleted mutants. The purified HFB was dissolved in water for enzyme activity assays.

Synthesis of Tricarballylic Acid Monothioesters. *N*-Acetylcysteamine (**1**) and phenyl (**2**) monothioesters of tricarballylic acid were prepared as illustrated in Figure 3 (experimental details are available in Supporting Information). Protection of cyclopentene acetic acid as the corresponding trichloroethyl ester was followed by oxidative cleavage of the alkene with ruthenium tetroxide. Thioesterification of the resulting diacid with *N*-acetylcysteamine and thiophenol cleanly produced the corresponding phenyl and SNAC monothioesters. Reductive deprotection of the trichloroethyl esters furnished the tricarballylic monothioesters. As the phenyl thioester decomposed rapidly following dissolution in neutral buffers, the biosynthetic studies were conducted with the *N*-acetylcysteamine thioester, which was indefinitely stable.

Activity Assays for Fum14p. A typical assay solution (100 µL) contained 2 mM tricarballylic thioester, 0.1 mM HFB (HFB$_1$, HFB$_3$, or HFB$_4$), 2.3 µM Fum14p, and 5 mM $MgCl_2$, in 100 mM Tris-HCl buffer, pH 7.4. Reactions without Fum14p were used as controls. After 30 min incubation at 37 °C, the reactions were stopped by the addition of 0.2 mL of cold 100% ethanol. After 30 min on ice, the precipitated protein was removed by centrifugation at 13 200 rpm at 4 °C for 20 min, and the supernatant was transferred to a new tube and dried under vacuum. Finally, the residues in the tube were redissolved in 50 µL of water for HPLC−ELSD and LC−ESIMS analysis.

HPLC−ELSD and ESIMS Analysis. The HPLC system was a ProStar, model 210 from Varian (Walnut Creek, CA) with an Alltima C18LL column (250 mm × 4.6 mm i.d., 5µm, Alltech, Deerfield, IL). The mobile phases were (A) water−TFA (100:0.025, v/v) and (B) acetonitrile−TFA (100:

0.025, v/v) with a gradient of 0−40% B in A in the first 10 min, 40−80% B in A from 10 to 15 min, 80% B in A from 15 to 20 min, 80−100% B in A from 20 to 21 min, 100% B in A from 21 to 23 min, and 100−0% B in A from 23 to 25 min. The flow rate was 1.0 mL/min, and a 50 µL sample was injected. The conditions set for light-scattering detection using an ELSD2000 (Alltech, Deerfield, IL) were the same as described previously (*22*). For preparative HPLC, the respective fractions were collected directly from the column according to their retention times. ESIMS was carried out on an API Qtrap 4000. The samples were directly infused in the mass spectrometer and analyzed in positive ion mode using Turbo Ion Spray Source.

RESULTS

FUM14-Deleted Mutants Produced HFB$_3$ and HFB$_4$. The transformation of *F. verticillioides* protoplasts with pUCH2-F14 resulted in 33 colonies that were able to grow on YPD plates containing hygromycin B. The resistance phenotype of these transformants was confirmed by the growth of the individual colonies in liquid YPD medium containing a high concentration (300 µg/mL) of hygromycin B. The genomic DNA isolated from the 33 transformants was then used in PCR screening for *FUM14*-deleted mutants. When primers P1/P2 were used, PCR of 12 transformants yielded a 1.4 kb fragments, which is expected to result from a homologous recombination of the left-side arm sequence in pUCH2-F14 and the *F. verticillioides* genome (Figure 2B). The 12 colonies were further screened by PCR using primers P3/P4. Except for one transformant, all transformants clearly yielded a 1.3 kb fragment, which is expected to result from a homologous recombination at the right-side arm sequence in pUCH2-F14 and the *F. verticillioides* genome (Figure 2B). To further verify the identity of the transformants, the PCR products from four representative transformants (number 23, 27, 31, and 33) were digested with *Kpn*I and *Eco*RI. Two fragments, 693 and 796 bp, were produced when the PCR product amplified by primer P1/P2 was digested with *Kpn*I, whereas three fragments, 754, 446, and 141 bp, were generated when the PCR product amplified by primers P3/P4 was digested with *Eco*RI (data not shown). The presence of *HygB* in each of the transformants was further verified by PCR amplification of the gene from the genomic DNA of the transformants, with the wild-type strain as a negative control (data not shown). Together, the results showed that we have obtained at least four fungal strains that are *FUM14*-deleted mutants, in which the coding region of *FUM14* was replaced with *HygB* (Figure 2B). The four mutants were used in the subsequent experiments for the production and analysis of metabolites.

After 3 weeks of growth in CMK medium, the wild-type progenitor strain produced B-series fumonisins, FB$_1$, FB$_2$, FB$_3$, and FB$_4$, with retention times of 16.2, 17.0, 17.2, and 18.1 min, respectively, on HPLC−ELSD (Figure 4A). The extracts from *FUM14*-deleted mutants gave three main peaks on HPLC−ELSD, with retention times of 16.1, 16.9, and 18.1 (Figure 4B). Since the retention times are very close to those from the wild-type strain, the extract from the wild-type strain was combined with the extract from the mutant and re-injected to HPLC. Two groups of peaks, with each approximately corresponding to that of the wild-type strain or of the mutant, were produced on HPLC−ELSD (data not
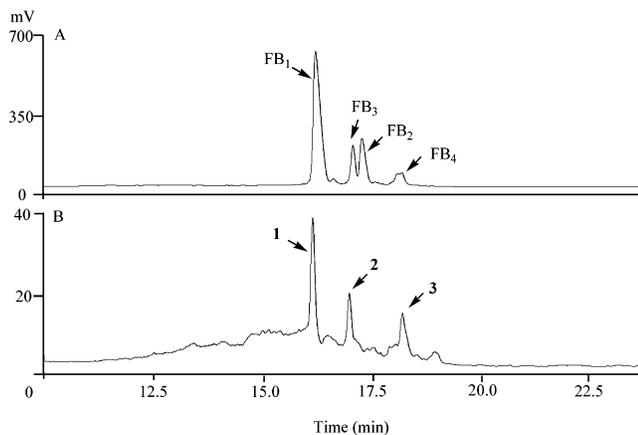
FIGURE 4: HPLC−ELSD analysis of metabolites produced in *F. verticillioide*. (A) wild-type; (B) *FUM14* deletion mutant. The identity of the peaks on the wild-type panel is indicated.

shown). The results suggest that the peaks in the extract from mutants correspond to compounds that differ from fumonisins produced by the wild-type progenitor strain. In the similar spiking experiments, Peak-1 of the mutant extract did not comigrate with standard HFB_1. However, Peak-2 and Peak-3 comigrated with standard HFB_3 and HFB_4 (data not shown). The three peaks were collected individually and analyzed by ESIMS. Peak-1 exhibited a yellowish color and gave several molecular ions, among which were $[M + H]^+$ of 321.3 *m/z* for methylfusarubin and 303.3 and 337.4 *m/z* for the dehydrolyzed form and hydroxylated form of methylfusarubin, respectively (*23*). These pigments have been observed in other *FUM*-deleted mutants and are not related to fumonisins (Yu, F. and Du, L., unpublished observations). Peak-2 gave only one clear molecular ion of 390.6 *m/z*, which is identical to standard HFB_3. Peak-3 contained a predominant molecular ion of 374.6 *m/z*, which is the same as standard HFB_4. The results from HPLC and ESIMS show that *FUM14*-deleted mutants produce two hydrolyzed fumonisins, HFB_3 and HFB_4, but not fumonisins HFB_1 or HFB_2.

Production of Fum14p-C and Fum14p in E. coli. FUM14 was initially predicted to encode only for a condensation domain of NRPS (*11*). Results from the recent EST sequencing project of *F. verticillioides* showed that the start codon of *FUM14* is located upstream of the previously predicted start codon (*24*). We found that the amino acid sequence deduced from this new coding region is similar to two domains within NRPS, a PCP domain at the N-terminus and a condensation domain at the C-terminus. The highly conserved 4′-phosphopantetheinyl binding motif, FFDLG-GDSVKA (consensus sequence GGxS; serine residue being the 4′-phosphopantetheinyl binding site), is found in the PCP domain of Fum14p, whereas the conserved motifs, including the C3 motif DHTHCDAFSR (typical consensus sequence HHxxxDG), are found in the C domain of Fum14p (Figure 5) (*13, 16*).

We constructed expression vectors for Fum14p C domain alone (Fum14p-C) as well as for the entire protein (Fum14p). The corresponding regions of *FUM14* were initially cloned into expression vector pET28a under control of a T7/*lac* promoter. The proteins were overproduced in *E. coli* strain BL21(DE3) upon IPTG induction. However, the produced proteins were totally insoluble under all conditions tested.

The Fum14p- and Fum14p-C-coding regions were then moved to the yeast expression system, pYES/NT, in the INVSc1 strain (Invitrogen). However, the expression level of both proteins was so extremely low that neither was purified from this system. Finally, we moved the Fum14p- and Fum14p-C-coding regions to the TB2/pMALc2 system to test whether the proteins could be expressed as soluble proteins when fused to MBP. Although the expression level was lower than in the BL21(DE3)/pET28a, the produced proteins appeared partially soluble. The proteins were purified on an amylose affinity column. The single domain protein, produced from the Fum14p-C coding region, yielded a band at approximately the 90 kDa region on SDS−PAGE (Figure 5A), which is consistent with the expected size for the fusion protein (92.5 kDa). The entire Fum14p protein, produced from the intact Fum14p coding region, yielded a band at approximately the 100 kDa region on SDS−PAGE (Figure 5B), which is in agreement with the expected size for the fusion protein (104.8 kDa).

Esterification of HFB_3 and HFB_4 by Fum14p. Fum14p was initially tested for the ability to transfer commercially available acyl-CoA, including acetyl-CoA, malonyl-CoA, and succinyl-CoA, to hydrolyzed fumonisins. However, none of the acyl-CoA appeared to serve as substrate for the enzyme. Subsequently, we chemically synthesized the SNAC monothioester of tricarballylic acid as substrate mimic. Since HFB_3 was the major metabolite accumulated in the *FUM14* mutant, we first tested the activity of Fum14p using HFB_3 as the acceptor substrate and TCA-SNAC as the acyl donor. HPLC analysis of the reaction mixture showed the presence of a major peak at 16.93 min (Peak-1 in Figure 6C), which comigrated with standard HFB_3, and a smaller peak at 16.99 min (Peak-2 in Figure 6C), which comigrated with standard FB_3. Peak-2 was not observed in the control where Fum14p was omitted in the reaction (Figure 6B). To confirm the formation of FB_3 in the reaction, the reaction mixture was subjected to ESIMS analysis. A clear molecular ion of 706.7 *m/z*, which was identical to standard FB_3, was detected, in addition to the 390.6 *m/z* ion for standard HFB_3. Only the 390.6 *m/z* ion, but not the 706.7 *m/z* ion, was present in the corresponding fraction collected from the control reaction. We also tested the activity of Fum14p using HFB_4 as the acceptor and TCA-SNAC as the donor. HPLC analysis of the reaction mixture showed a single peak at 18.10 min, which comigrated with standard HFB_4 (data not shown). Because FB_4 and HFB_4 have the same retention time under the experimental conditions, we analyzed the reaction mixture by ESIMS. The results showed that a 690.8 *m/z* ion, which was identical to standard FB_4, was present in the fraction from the reaction, but not from the control in which Fum14p was not included. The control contained only the 374.6 *m/z* ion for HFB_4. The results show that Fum14p is able to esterify HFB_3 and HFB_4 using TCA-SNAC as the acyl donor to produce the corresponding fumonisins. Finally, we tested the activity of the C domain (Fum14p-C) using HFB_3 or HFB_4 as the acceptor. The results from HPLC and ESIMS analysis suggest that no fumonisin was formed in the reactions (data not shown).

Esterification of HFB_1 by Fum14p and Fum14p-C. To obtain information about the specificity of Fum14p toward the acceptor substrate, we further tested the esterification of

C3 motif of C-domain			
HTS1	1479	NHLVFDGMST	1488
HMWP2	245	DLLIMDASSF	254
EntF	136	HHLLVDGFSF	145
Fum14p	244	DHTHCDAFSR	253

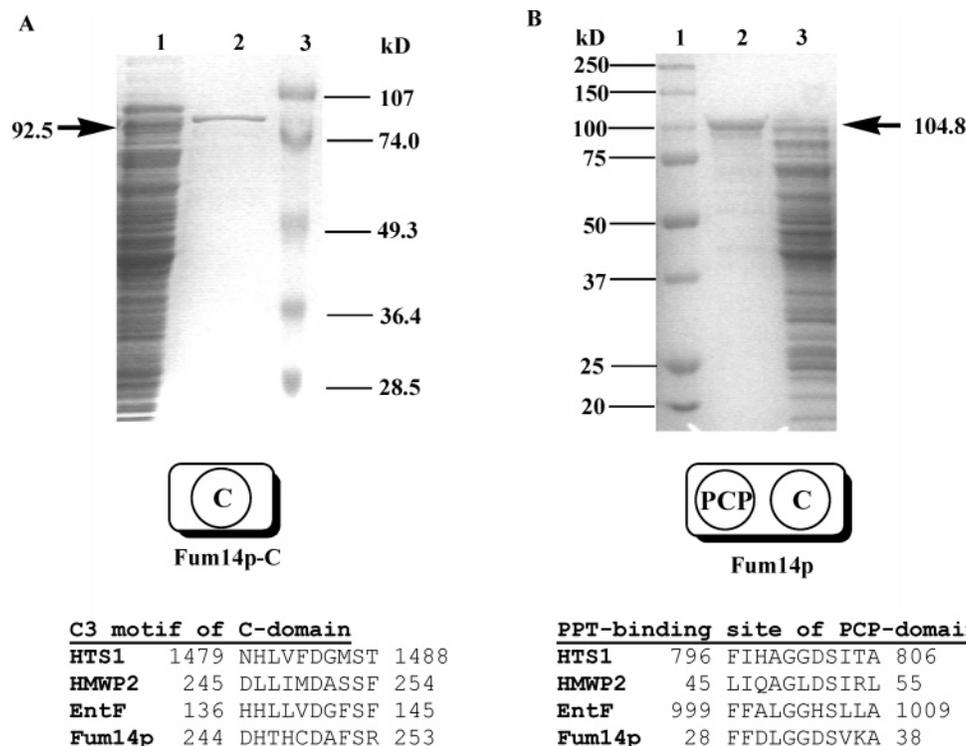| PPT-binding site of PCP-domain			
HTS1	796	FIHAGGDSITA	806
HMWP2	45	LIQAGLDSIRL	55
EntF	999	FFALGGHSLLA	1009
Fum14p	28	FFDLGGDSVKA	38

FIGURE 5: Sodium dodecyl sulfate−polyacrylamide gel analysis of Fum14p expressed in *E. coli*. (A) The condensation domain of Fum14p. lane 1, total soluble proteins; lane 2, purified protein; lane 3, protein size markers. (B) Intact Fum14p. Lane 1, protein size markers; lane 2, purified protein; lane 3, total soluble proteins. The conserved motif for the condensation domain and peptidyl carrier protein of nonribosomal peptides is listed under the SDS−PAGE. HTS1, HC-toxin synthetase (Q01886) from *Cochliobolus carbonum*; HMWP2, high-molecular-weight protein 2 (P48633) from *Yersinia enterocolitica*; EntF, enterobactin synthetase component F (P11454) from *E. coli*.
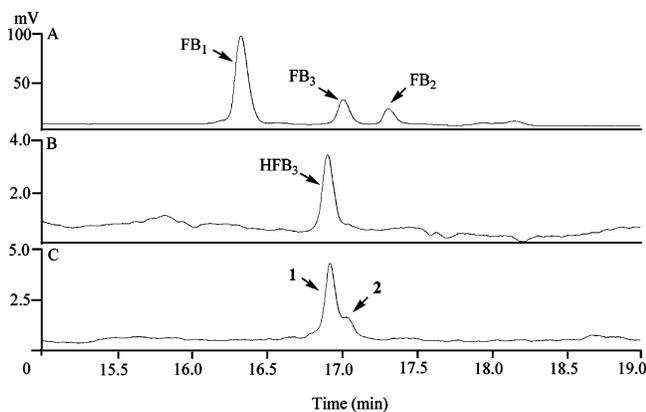

FIGURE 6: HPLC−ELSD analysis of the reaction catalyzed by Fum14p using HFB$_3$ as substrate in the presence of TCA thioester. (A) Standard FB$_1$, FB$_2$, and FB$_3$; (B) standard HFB$_3$; (C) reaction mixture.
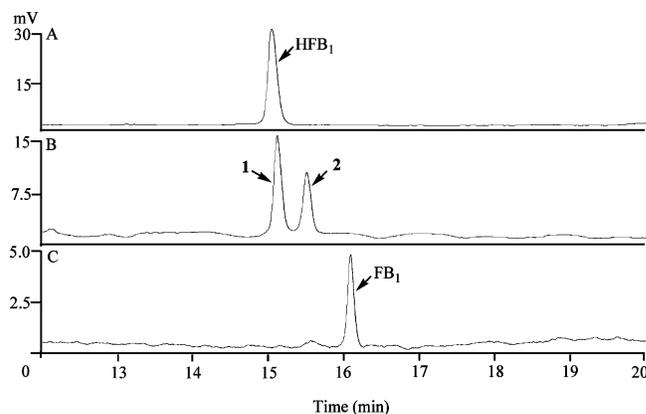
FIGURE 7: HPLC−ELSD analysis of the reaction catalyzed by Fum14p using HFB$_1$ as substrate in the presence of TCA thioester. (A) Standard HFB$_1$; (B) reaction mixture; (C) standard FB$_1$.

HFB$_1$, which is the hydrolyzed form of FB$_1$ but that was not detected in extracts of *FUM14* deletion mutants (see Figure 4). HFB$_1$ contains one more hydroxyl (C-5 hydroxyl) than HFB$_3$ and two more hydroxyl (C-5 and C-10 hydroxyl) than HFB$_4$. Reactions that included HFB$_1$, the thioester TCA−SNAC, and the intact enzyme Fum14p yielded two peaks upon HPLC analysis, one peak at 15.0 min (Peak-1) and the other at 15.6 min (Peak-2) (Figure 7B). Peak-1 comigrated with standard HFB$_1$ (Figure 7A), but Peak-2 did not comigrate with standard FB$_1$, which had a retention time of 16.1 min (Figure 7C). ESIMS analysis revealed that the reaction mixture contained a new product with a [M + H]$^+$ ion of 564.2 *m/z*, in addition to HFB$_1$, which has a [M + H]$^+$ ion of 406.5 *m/z*. The product with

a [M + H]$^+$ ion of 564.2 *m/z* is coincident with PHFB$_1$, the partly hydrolyzed FB$_1$ that contains only one of the two tricarballylic esters of FB$_1$ (*25*). It is not clear at this time which regioisomer (C-14 ester or C-15 ester) of PHFB$_1$ might be formed in the reaction. When the C domain (Fum14p-C) was used in the reaction instead of the intact protein, two peaks were also detected on HPLC (Figure 8B). The first peak (Peak-2) comigrated with PHFB$_1$, whereas the second peak (Peak-3) comigrated with FB$_1$ (Figure 8C). The identity of the two peaks was confirmed by ESIMS. The [M + H]$^+$ for Peak-2 was 564.6 *m/z*, which is identical to that for PHFB$_1$, and the [M + H]$^+$ for Peak-3 was 722.7 *m/z*, which is identical to that for FB$_1$. The results show that both the Fum14p and Fum14p-C proteins were able to esterify HFB$_1$ in vitro.
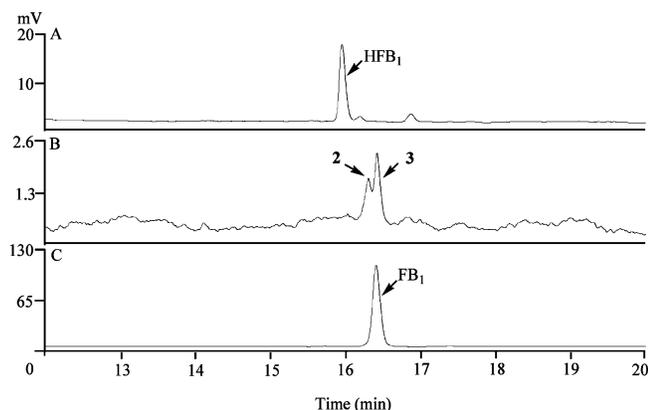
FIGURE 8: HPLC−ELSD analysis of the reaction catalyzed by the condensation domain of Fum14p using HFB_1 as substrate in the presence of TCA thioester. (A) Standard HFB_1; (B) reaction mixture; (C) standard FB_1.

DISCUSSION

Typical NRPS are modular enzymes, with each module (except initiation module and termination module) minimally containing three domains, the adenylation domain, PCP, and the condensation domain (*13, 16*). The enzymes are multifunctional complexes consisting of several modules in a single polypeptide. For example, the NRPS cyclosporine A synthetase includes 11 modules (*26*). *FUM14* is predicted to encode an NRPS with only the PCP and C domains. To define the role of *FUM14* in fumonisin biosynthesis, we generated *FUM14* deletion mutants of *F. verticillioides*, in which the protein coding region of *FUM14* was replaced with a hygromycin resistance gene. This approach was used previously to define the function of other *FUM* genes (*20,*

27, 28). HPLC and ESIMS analysis of extracts of the *FUM14* deletion mutants revealed that the mutants did not produce any of the typical B-series fumonisins FB_1, FB_2, FB_3, and FB_4. Instead, the mutants produced pre-fumonisins, HFB_3 and HFB_4, which are identical to FB_3 and FB_4, respectively, except that they lack the TCA ester functions. The fact that the mutants lost the ability to produce the TCA-esterified fumonisins indicates that *FUM14* is involved in the esterification of fumonisins. The results are consistent with the preliminary observations determined previously (*12*). The absence of partly esterified products (PHFB) in the mutant extracts suggests that *FUM14* is responsible for the TCA esters at both C-14 and C-15 of the fumonisin backbone.

PCP and C domains of NRPS have not been reported previously to catalyze the formation of the C−O bone of ester functions. Thus, the PCP and C domains of Fum14p could be unusual in their activity. To further characterize this unusual activity, we conducted a heterologous expression analysis of Fum14p. This analysis has been challenging due to the difficulty in the heterologous expression of the genes from *F. verticillioides* (*29, 30*). We were able to express *FUM14* in *E. coli* and purify the protein to near homogeneity only after it was fused to maltose binding protein (MBP). The in vitro assays showed that the intact enzyme was able to convert HFB_3 to FB_3 and HFB_4 to FB_4, using TCA thioester as the acyl donor. The results have two important implications. First, the biochemical data provide direct evidence for the function of Fum14p, that is, that it catalyzes the esterification of TCAs to both C-14 and C-15 of the fumonisin backbone. The biochemical data are also consistent with the results from the *FUM14* deletion analysis. *FUM14* represents the third gene among the 15-gene cluster for
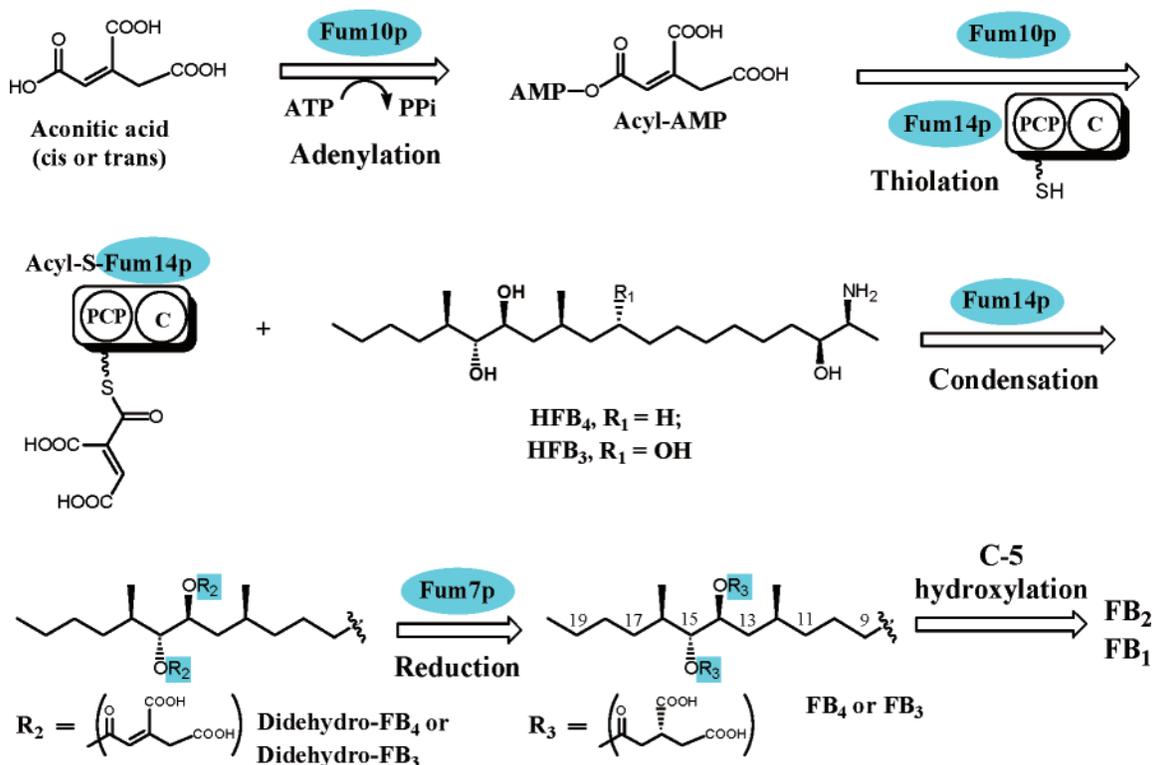

FIGURE 9: A proposed mechanism for the NRPS-catalzyed tricarballylic ester formation of fumonisins. Note that an unsaturated tricarboxylate, such as aconitic acid, is proposed to be the origin of the tricarballylic esters in vivo. Three *FUM* genes, *FUM10*, *FUM14*, and *FUM7*, together code for a four-domain NRPS complex to catalyze the adenylation, thiolation, condensation, and reduction of the tricarballylic esters of fumonisins.

biosynthesis of fumonisins that has been biochemically characterized (*29, 30*). Because of the importance of the esters in the fumonisin toxicity, it is significant to define the genetic and biochemical basis of their formation. Second, the in vitro data demonstrate the first example of NRPS-catalyzed C−O bond formation. Fum14p contains PCP and C domain, in which the C domain is the catalytic unit according to the paradigm of NRPS-catalyzed reactions (*13, 16*). In typical NRPS, the C domain catalyzes the condensation reaction of a peptidyl-*S*-PCP and an aminoacyl-*S*-PCP to produce a new amide bond (*13, 16*). The substrates are covalently linked to the enzyme via the 4′-phosphopantetheinyl group of the PCP domain. Acyl-SNAC is a mimic of acyl-*S*-PCP, which is commonly used as substrate in the in vitro studies of NRPS and polyketide synthases (*31, 32*). In its natural environment, Fum14p is predicted to catalyze a condensation reaction between an enzyme-bound substrate (TCA-SNAC mimic) and a free substrate (hydrolyzed FB) to form an ester bond. It is noteworthy that the C domain alone (Fum14p-C) appeared inactive when HFB_3 or HFB_4 was used as the substrate, but active when HFB_1 was the substrate. The reason for the difference is not clear but could be related to the C-5 hydroxyl group on HFB_1 that may provide a favorable interaction with the enzyme. The fact that HFB_1 was converted to $PHFB_1$ and FB_1 by Fum14p-C shows that the removal of the PCP domain did not lead to an inactive enzyme.

Three genes, *FUM7*, *FUM10*, and *FUM14*, have been suggested to be involved in the esterification of fumonisins (*12*). The genes together may encode an NRPS complex. *FUM10* is similar to genes coding for the adenylation domains of NRPS, whereas *FUM14* encodes the PCP and condensation domain of NRPS. *FUM7* is similar to genes for dehydrogenases/reductases, which could be regarded as a reductase (R) domain of NRPS. Together, the genes could encode a four-domain NRPS complex, A−PCP−C−R. On the basis of the data obtained from this study and previous studies (*11, 12*), we propose a mechanism for the biosynthesis of the TCA esters of fumonisins (Figure 9). The first step is the ATP-dependent activation of a tricarboxylate substrate by Fum10p to form an acyl-AMP, which is subsequently transferred to the PCP domain of Fum14p. The exact substrate for Fum10p is not known yet, but was suggested to be an intermediate of the Krebs Cycle (*10*). Preliminary data obtained from the disrupted mutants of *FUM10* and *FUM7* suggested that the substrate of Fum10p could be a tricarboxylate containing a double bond (*12*), such as aconitic acid (Figure 9). The second step is the C domain-catalyzed condensation between acyl-*S*-PCP of Fum14p and HFB_3 or HFB_4 to produce a didehydro-intermediate of FB_3 or FB_4, respectively. If this is the case, the direct substrate in vivo for the C domain could be an unsaturated tricarboxylate thioester, rather than the TCA thioester that we used in our enzyme assays in vitro. Attempts to chemically synthesize a monothioester of aconitic acid as an unsaturated analog of TCA-SNAC have been frustrated by the difficulties of dealing with the reactive functionality in the molecule (Xu, C. and Dussault, P. H., unpublished results). The last step is the reduction of the double bond in the didehydro-intermediate by Fum7p to produce FB_3 and FB_4 (Figure 9). A hydroxylation at carbon-5 will convert FB_3 and FB_4 to FB_1 and FB_2, respectively. This step is believed to be the last

step in the whole biosynthetic pathway and has been characterized (*27, 29*). We are currently working on the characterization of Fum10p and Fum7p to provide further evidence for the proposed mechanism for esterification of fumonisins.

ACKNOWLEDGMENT

SUPPORTING INFORMATION AVAILABLE

Procedures for the synthesis of tricarballylic acid monothioesters, *N*-acetylcysteamine (**1**) and phenyl (**2**) monothioesters of tricarballylic acid. This material is available free of charge via the Internet at http://pubs.acs.org.

REFERENCES

1. Marasas, W. F. (2001) Discovery and occurrence of the fumonisins: a historical perspective, *Environ. Health Perspect. 109* (Suppl. 2), 239−243.
2. Nelson, P. E., Desjardins, A. E., and Plattner, R. D. (1993) Fumonisins, mycotoxins produced by *Fusarium* species: biology, chemistry, and significance, *Annu. Rev. Phytopathol. 31*, 233−252.
3. Merrill, A. H., Jr., van Echten, G., Wang, E., and Sandhoff, K. (1993) Fumonisin B1 inhibits sphingosine (sphinganine) *N*-acyltransferase and de novo sphingolipid biosynthesis in cultured neurons in situ, *J. Biol. Chem. 268*, 27299−27306.
4. Gelderblom, W. C., Jaskiewicz, K., Marasas, W. F., Thiel, P. G., Horak, R. M., Vleggaar, R., and Kriek, N. P. (1988) Fumonisins—novel mycotoxins with cancer-promoting activity produced by *Fusarium moniliforme*, *Appl. Environ. Microbiol. 54*, 1806−1811.
5. Marasas, W. F., Kellerman, T. S., Gelderblom, W. C., Coetzer, J. A., Thiel, P. G., and van der Lugt, J. J. (1988) Leukoencephalomalacia in a horse induced by fumonisin B1 isolated from *Fusarium moniliforme*, *Onderstepoort J. Vet. Res. 55*, 197−203.
6. Bezuidenhout, S. C., Gelderblom, W. C. A., Gorst-Allman, C. P., Horak, R. M., Marasas, W. F. O., Spiteller, G., and Vleggaar, R. (1988) Structure elucidation of the fumonisins, mycotoxins from *Fusarium moniliforme*, *J. Chem. Soc. Chem. Commun.* 743−745.
7. Seefelder, W., Humpf, H. U., Schwerdt, G., Freudinger, R., and Gekle, M. (2003) Induction of apoptosis in cultured human proximal tubule cells by fumonisins and fumonisin metabolites, *Toxicol. Appl. Pharmacol. 192*, 146−153.
8. Yin, J. J., Smith, M. J., Eppley, R. M., Troy, A. L., Page, S. W., and Sphon, J. A. (1996) Effects of fumonisin B1 and (hydrolyzed) fumonisin backbone AP1 on membranes: a spin-label study, *Arch. Biochem. Biophys. 335*, 13−22.
9. Humpf, H. U., Schmelz, E. M., Meredith, F. I., Vesper, H., Vales, T. R., Wang, E., Menaldino, D. S., Liotta, D. C., and Merrill, A. H., Jr. (1998) Acylation of naturally occurring and synthetic 1-deoxysphinganines by ceramide synthase. Formation of *N*-palmitoyl-aminopentol produces a toxic metabolite of hydrolyzed fumonisin, AP1, and a new category of ceramide synthase inhibitor, *J. Biol. Chem. 273*, 19060−19064.
10. Blackwell, B. A., Edwards, O. E., Fruchier, A., ApSimon, J. W., and Miller, J. D. (1996) NMR structural studies of fumonisin B1 and related compounds from *Fusarium moniliforme*, *Adv. Exp. Med. Biol. 392*, 75−91.
11. Proctor, R. H., Brown, D. W., Plattner, R. D., and Desjardins, A. E. (2003) Co-expression of 15 contiguous genes delineates a fumonisin biosynthetic gene cluster in *Gibberella moniliformis*, *Fungal Genet. Biol. 38*, 237−249.
12. Butchko, R. A., Plattner, R. D., and Proctor, R. H. (2003) Esterification of tricarballylic acid side chains to the fumonisin backbone requires the activity of four *FUM* genes, presented at the Aflatoxin/Fumonisin Elimination and Fungal Genomics Workshop, Savannah, GA.
13. Marahiel, M. A., Stachelhaus, T., and Mootz, H. D. (1997) Modular peptide synthetases involved in nonribosomal peptide synthesis, *Chem. Rev. 97*, 2651−2674.
14. Reimmann, C., Patel, H. M., Serino, L., Barone, M., Walsh, C. T., and Haas, D. (2001) Essential PchG-dependent reduction in

pyochelin biosynthesis of *Pseudomonas aeruginosa*, *J. Bacteriol. 183*, 813−820.

15. Patel, H. M., and Walsh, C. T. (2001) In vitro reconstitution of the *Pseudomonas aeruginosa* nonribosomal peptide synthesis of pyochelin: characterization of backbone tailoring thiazoline reductase and *N*-methyltransferase activities, *Biochemistry 40*, 9023−9031.

16. Walsh, C. T., Gehring, A. M., Weinreb, P. H., Quadri, L. E., and Flugel, R. S. (1997) Post-translational modification of polyketide and nonribosomal peptide synthases, *Curr. Opin. Chem. Biol. 1*, 309−315.

17. Sambrook, J., Fritsch, E. F., and Maniatis, T. (1989) *Molecular Cloning: A Laboratory Manual*, 2nd ed., Cold Spring Harbor Laboratory Press, New York.

18. Desjardins, A. E., Plattner, R. D., and Proctor, R. H. (1996) Genetic and biochemical aspects of fumonisin production, *Adv. Exp. Med. Biol. 392*, 165−173.

19. Turgeon, B. G., Garber, R. C., and Yoder, O. C. (1987) Development of a fungal transformation system based on selection of sequences with promoter activity, *Mol. Cell. Biol. 7*, 3297−3305.

20. Yu, F., Zhu, X., and Du, L. (2005) Developing a genetic system for functional manipulations of *FUM1*, a polyketide synthase gene for the biosynthesis of fumonisins in *Fusarium verticillioides*, *FEMS Microbiol. Lett. 248*, 257−264.

21. Hartl, M., and Humpf, H. U. (1999) Simultaneous determination of fumonisin B(1) and hydrolyzed fumonisin B(1) in corn products by liquid chromatography/electrospray ionization mass spectrometry, *J. Agric. Food Chem. 47*, 5078−5083.

22. Bojja, R. S., Cerny, R. L., Proctor, R. H., and Du, L. (2004) Determining the biosynthetic sequence in the early steps of the fumonisin pathway by use of three gene-disruption mutants of *Fusarium verticillioides*, *J. Agric. Food Chem. 52*, 2855−2860.

23. Kurobane, I., Zaita, N., and Fukuda, A. (1986) New metabolites of *Fusarium martii* related to dihydrofusarubin, *J. Antibiot. 39*, 205−214.

24. Brown, D. W., Cheung, F., Proctor, R. H., Butchko, R. A., Zheng, L., Lee, Y., Utterback, T., Smith, S., Feldblyum, T., Glenn, A. E., Plattner, R. D., Kendra, D. F., Town, C. D., and Whitelaw, C. A. (2005) Comparative analysis of 87,000 expressed sequence tags from the fumonisin-producing fungus *Fusarium verticillioides*, *Fungal Genet. Biol. 42*, 848−861.

25. Rheeder, J. P., Marasas, W. F., and Vismer, H. F. (2002) Production of fumonisin analogs by *Fusarium* species, *Appl. Environ. Microbiol. 68*, 2101−2105.

26. Weber, G., Schorgendorfer, K., Schneider-Scherzer, E., and Leitner, E. (1994) The peptide synthetase catalyzing cyclosporine production in *Tolypocladium niveum* is encoded by a giant 45.8-kilobase open reading frame, *Curr. Genet. 26*, 120−125.

27. Butchko, R. A., Plattner, R. D., and Proctor, R. H. (2003) *FUM9* is required for C-5 hydroxylation of fumonisins and complements the meitotically defined Fum3 locus in *Gibberella moniliformis*, *Appl. Environ. Microbiol. 69*, 6935−6937.

28. Butchko, R. A., Plattner, R. D., and Proctor, R. H. (2003) *FUM13* encodes a short chain dehydrogenase/reductase required for C-3 carbonyl reduction during fumonisin biosynthesis in *Gibberella moniliformis*, *J. Agric. Food Chem. 51*, 3000−3006.

29. Ding, Y., Bojja, R. S., and Du, L. (2004) Fum3p, a 2-ketoglutarate-dependent dioxygenase required for C-5 hydroxylation of fumonisins in *Fusarium verticillioides*, *Appl. Environ. Microbiol. 70*, 1931−1934.

30. Yi, H., Bojja, R. S., Fu, J., and Du, L. (2005). Direct evidence for the function of *FUM13* in 3-ketoreduction of mycotoxin fumonisins in *Fusarium verticillioides*, *J. Agric. Food Chem. 53*, 5456−5460.

31. Ehmann, D. E., Trauger, J. W., Stachelhaus, T., and Walsh, C. T. (2000) Aminoacyl-SNACs as small-molecule substrates for the condensation domains of nonribosomal peptide synthetases, *Chem. Biol. 7*, 765−772.

32. Cane, D. E., Kudo, F., Kinoshita, K., and Khosla, C. (2002) Precursor-directed biosynthesis: biochemical basis of the remarkable selectivity of the erythromycin polyketide synthase toward unsaturated triketides, *Chem. Biol. 9*, 131−142.